

TSOM Method for Semiconductor Metrology

Ravikiran Attota**, Ronald G. Dixson, John A. Kramar, James E. Potzick, András E. Vladár,
Benjamin Bunday*, Erik Novak[#], and Andrew Rudack*

National Institute of Standards and Technology, Gaithersburg, MD 20899, USA

*SEMATECH, Albany, NY 12203, USA

[#] Bruker Nano Surfaces Division, Tucson, AZ 85756, USA

ABSTRACT

Through-focus scanning optical microscopy (TSOM) is a new metrology method that achieves 3D nanoscale measurement sensitivity using conventional optical microscopes; measurement sensitivities are comparable to what is typical when using scatterometry, scanning electron microscopy (SEM), and atomic force microscopy (AFM). TSOM can be used in both reflection and transmission modes and is applicable to a variety of target materials and shapes. Nanometrology applications that have been demonstrated by experiments or simulations include defect analysis, inspection and process control; critical dimension, photomask, overlay, nanoparticle, thin film, and 3D interconnect metrologies; line-edge roughness measurements; and nanoscale movements of parts in MEMS/NEMS. Industries that could benefit include semiconductor, data storage, photonics, biotechnology, and nanomanufacturing. TSOM is relatively simple and inexpensive, has a high throughput, and provides nanoscale sensitivity for 3D measurements with potentially significant savings and yield improvements in manufacturing.

Keywords: TSOM, through focus, optical microscope, nanometrology, process control, nanomanufacturing, nanoparticles, overlay metrology, critical dimension, defect analysis, dimensional analysis, MEMS, NEMS, photonics

1. INTRODUCTION

The demand on tools to make 3D measurements at the nanoscale is very high as dimensional information at the nanoscale is required to enable progress in nanotechnology and nanoscience [1,2]. Several tools, such as the atomic force microscope (AFM), scanning tunneling microscope (STM), and scanning electron microscope (SEM) are routinely used to provide measurements at this scale. However, with the commercialization of nanotechnology, fast and reliable nanoscale feature measurements will become increasingly important [1,2]. Optics-based tools can be advantageous because they have a relatively low cost of ownership with high throughput, and are usually completely non-contaminating and non-destructive.

It is often a misconception that optical microscopes are not well suited for dimensional measurements of features that are smaller than half the wavelength of illumination (200 nm sized features in the visible region) due to diffraction [3]. Of course, optical microscopes have been used for years to measure photomask linewidth features that are well below half the illumination wavelength through experiment to model comparisons. Certainly, diffraction-dominated images make meaningful analysis of the targets difficult. However, this limitation can be circumvented by (i) considering the image as a dataset (or signal) that represents the target, (ii) using a set of through-focus images instead of one “best focus” image, and (iii) making use of highly developed optical models [4-6].

** Corresponding author : ravikiran.attota@nist.gov; phone: 1 301 975 5750

In conventional optical microscopy, images usually must be acquired at the "best focus" position for a meaningful analysis, based on the belief that the most faithful single image representation of the target is rendered only at the best focus position. However, the out-of-focus images do contain additional useful information about the target. This information can be obtained using an appropriate data acquisition and analysis method. Based on this and on the observation of a distinct signature for different parametric variations, we introduced a new method for nanoscale dimensional analysis with nanometer sensitivity for three-dimensional, nano-sized targets using a conventional brightfield optical microscope [7-14]: through-focus scanning optical microscopy (TSOM). TSOM is applicable to three-dimensional targets (where a single "best focus" may be impossible to define), thus enabling it to be used for a wide range of target geometries and application areas.

Through-focus optical information was used before for several applications. Most frequently it has been in use to find the best-focus image position. Contrast in the entire optical image is evaluated and plotted as a function of through-focus position. Image at the focus position corresponding to the maximum contrast is considered the best focus image.

Confocal microscopy is another method that makes use of through-focus optical image information. In this method, out-of-focus optical image information present in the through-focus images is selectively discarded to form a 3D confocal image. About 20 years ago, this microscopy was applied for overlay and CD analysis [15].

For line gratings it is not necessary to find the contrast in the entire image. It would be sufficient to evaluate contrast in a single trace cross-section across the lines. The intensity profile was reduced to a number by evaluating its contrast and plotted as a function of focus position. It was found that the through-focus contrast in the image of isolated line gratings was sensitive to the line width (CD) [16,17]. In these type of studies, the plot of contrast in the profile as a function of focus position was termed as "through-focus focus metric". CD analysis was performed by studying variations in the through-focus focus metric profile.

As a visual aid for CD analysis using through-focus focus metric, through-focus optical cross sectional intensity profiles were stacked to form an image similar to the 2D TSOM images used in the current study in Ref. [18].

Through-focus optical images were also used to study defects [19]. In this method, first through-focus optical images are obtained from a reference target and from targets containing defects. Optical images (not the cross sectional optical intensity profiles) from the reference and the defect targets at the same focus position are then subtracted to highlight defects or signal from defects in the 2D image. As will be seen in the following sections, TSOM method uses differential TSOM images (i.e differential cross sectional intensity images) as opposed to differential images as used in this defect analysis work.

In the TSOM method, through-focus images are stacked as a function of focus position resulting in a 3D space containing optical information. From this 3D image space, cross sectional 2D TSOM images are extracted through the location of interest in any given orientation. In the TSOM method the entire 3D optical information is acquired and preserved for dimensional analysis. Neither the out-of-focus optical information is discarded, as in Confocal microscopy, nor is the intensity profile reduced to a number, as in the through-focus focus metric method.

2. METHOD TO CONSTRUCT A TSOM IMAGE

The TSOM method requires a conventional brightfield optical microscope with a digital camera to capture images, and a motorized stage to move the target through the focus. Fig. 1 demonstrates the method to construct TSOM images using an isolated line as a target. Simulated optical images are used here to illustrate the method. Optical images are acquired as the target is scanned through the focus of the microscope (along the z -axis) as shown in Figs. 1(a) & 1(b). Each scan position results in a slightly different two-dimensional intensity image (Fig. 1(c)). The acquired optical images are stacked at their corresponding scan positions, creating a three-dimensional TSOM image, where the x and the y -axes represent the spatial position on the target and the z -axis the scanned focus position. In this 3D space, each location has a value corresponding to its optical intensity. The optical intensities in a plane (e.g., the xz plane) passing through the location of interest on the target (e.g., through the center of the line) can be conveniently plotted as a 2D image, resulting

in a 2D-TSOM image as shown in Fig. 1(e), where the x axis represents the spatial position on the target (in x), the y axis represents the focus position, and the color scale represents the optical intensity. Note that the intensity (color) axis is typically rescaled for each image. For 3D targets, appropriate 2D-TSOM images are selected for dimensional analysis. In this paper, we use “TSOM image” to refer to these 2D-TSOM cross-sectional images.

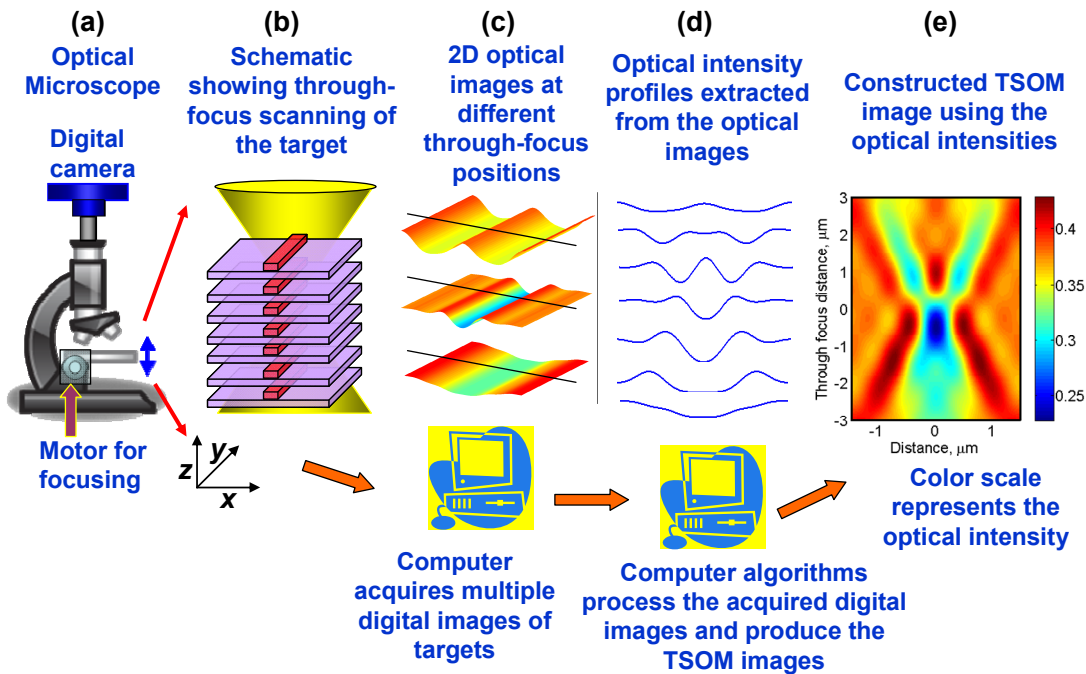


Figure 1. Method to construct TSOM images using a conventional optical microscope.

3. CHARACTERISTICS OF TSOM IMAGES

3.1 TSOM Images Change with Target

The TSOM images vary substantially for different types of targets. This variation is illustrated in Fig. 2 for four types of targets, using optical modeling simulations. An isolated line, measured using a reflection-based optical microscope, is shown in Fig. 2(a). A finite dense array with 9 lines produces the TSOM image in Fig. 2 (b). This target has a pitch of 105 nm, and the simulation was done using 193 nm. In-chip overlay targets must be small so that they can be placed in the active area. The TSOM image for an in-chip target at $\lambda = 193$ nm is shown in Fig. 2(c). A TSOM image may also be produced for transmission microscopy; a photomask target in a transmission mode microscope at $\lambda = 365$ nm is shown in Fig. 2(d). This target has a chrome line on a quartz substrate.

3.2 Differential TSOM Images Appear to be Distinct for Different Dimensional Changes

A small change in the dimension of a target produces a corresponding change in the TSOM image. Comparing two TSOM images from different targets, one can identify differences between the targets. Although one can compare and identify changes in different ways, here we present a method based on a differential TSOM image.

Although this method can be applied to any of the targets discussed in this paper, in the current analysis we demonstrate the approach for an isolated line (i.e., a line several wavelengths away from nearby features). The TSOM images were simulated for small differences in the target dimensions. Fig. 3 presents TSOM images for two targets with a 1.0 nm difference in the linewidth. Visual inspection of the two TSOM images would indicate that they are similar. In the same way, the TSOM images for a small difference in the line height or sidewall angle also appear similar. However, a

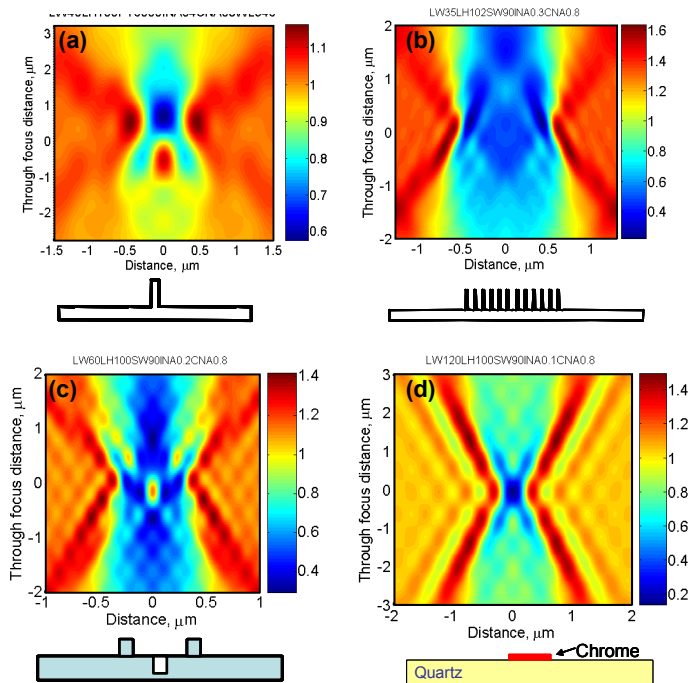


Figure 2. Simulated TSOM images for (a) an isolated Si line on a Si substrate (Line width = 40 nm, Line height = 100 nm, Illumination NA = 0.4, Collection NA = 0.8, and Illumination wavelength = 546 nm), (b) a finite dense Si array on a Si substrate (Number of lines = 9, Line width = 35 nm, Pitch = 105 nm, Line height = 100 nm, Illumination NA = 0.3, Collection NA = 0.8, and Illumination wavelength = 193 nm), (c) an in-chip Si line on a Si substrate overlay target (Linewidth = 60 nm, Line height = 100 nm, Trench width = 60 nm, Trench depth = 100 nm, Distance between the lines = 400 nm, Illumination NA = 0.2, Collection NA = 0.8, and Illumination wavelength = 193 nm), and (d) a chrome line on a quartz substrate photomask in transmission microscope mode (Linewidth = 120 nm, Line height = 100 nm, Illumination NA = 0.1, Collection NA = 0.8, Illumination wavelength = 365 nm).

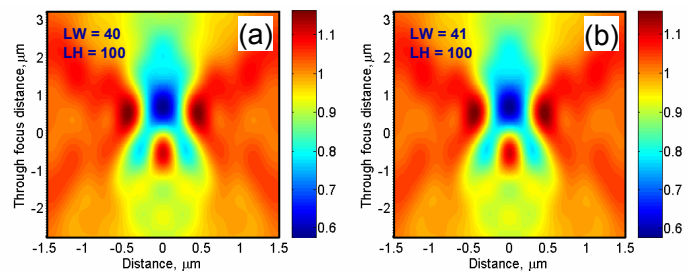


Figure 3. Simulated TSOM images for two isolated line targets. LW = Linewidth in nm, LH = Line height in nm, Illumination NA = 0.4, Collection NA = 0.8, Illumination wavelength = 546 nm, Si line on Si substrate.

simple subtraction of any two TSOM images distinctly highlights the difference between them. This difference can be illustrated using a differential TSOM image. The differential TSOM image is the difference in the optical intensities between any two similarly processed TSOM images. We analyzed the differential TSOM images for four different dimensional differences. They are a 1 nm difference in the line height, a 1 nm difference in the linewidth, a 1 nm difference in both the linewidth and the line height, and a 1 degree difference in the sidewall angle. The differential TSOM images for the four types of dimensional differences are shown in Fig. 4.

The following observations can be made from the differential TSOM images. For the simulations shown, a small change in the dimension of the target can be identified using this method. However, sensitivity to small dimensional changes will depend on the measurement noise, sensitivity, and monotonic response. The simulation data show that a small change in the line height, the linewidth, both the linewidth and the line height, or the sidewall angle show qualitatively distinct differential TSOM image responses. We have confirmed similar simulation-based results for several different types of targets. In Fig. 5, we present a second example for a finite dense line array. Again, we observe that individually the line height and the linewidth differences produce distinctive differential TSOM images. This simulation-based analysis demonstrates an intriguing possibility for identifying specific dimensional differences by examining differential TSOM images.

3.3 Differential TSOM Images are Qualitatively Similar for Differences in the Same Dimension

As shown above, different dimensional changes (i.e., width or height) produce qualitatively distinct differential TSOM images. However, for different magnitude changes of the same dimension, the differential TSOM images appear qualitatively similar. Figs 6(a) and (b) present differential TSOM images for 2.0 nm and 4.0 nm differences in linewidth, respectively, in an isolated line. Likewise, the differential TSOM images for 2.0 nm and 4.0 nm differences in the line heights of isolated lines are presented in Figs. 7(a) and (b), respectively. These simulations yield qualitatively similar appearing differential TSOM images. We performed the same analysis for several different types of

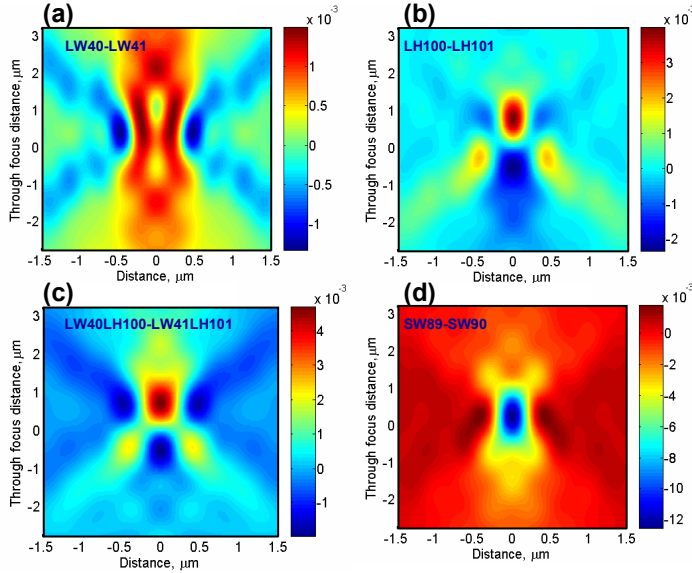


Figure 4. Simulated differential TSOM images obtained for the isolated lines shown in figure 4. (a) 1.0 nm change in the linewidth (b) 1.0 nm change in the line height (c) 1.0 nm change in both the line height and the linewidth, and (d) one degree change in the sidewall angle (LW = Linewidth in nm, LH = Line height in nm).

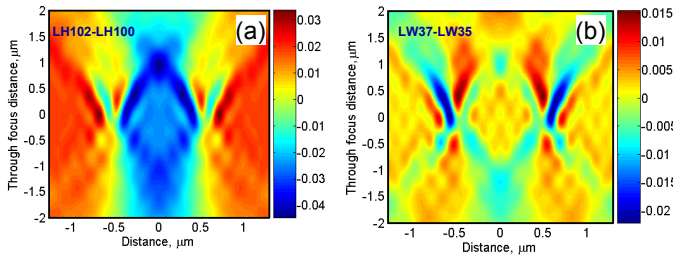


Figure 5. Simulated differential TSOM images obtained for finite dense arrays for (a) 2.0 nm change in the line height, and (b) 2.0 nm change in the linewidth. Linewidth = 35 nm, Line height = 100 nm, Illumination NA = 0.3, Collection NA = 0.8, Illumination wavelength = 193 nm, Si line on Si substrate.

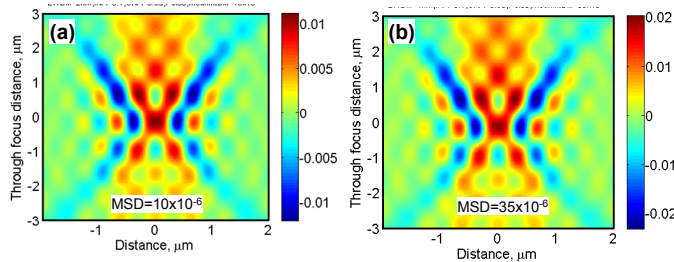


Figure 6. Simulated differential TSOM image obtained for (a) the linewidths of 102 nm and 100 nm (2.0 nm difference), and (b) the linewidths of 104 nm and 100 nm (4.0 nm difference). Isolated line, Line height = 100 nm, Illumination NA = 0.25, Collection NA = 0.95, Illumination wavelength = 546 nm, Si line on Si substrate.

targets under different conditions. In all the cases tested, we observed similar behavior, which holds true as long as the difference in the dimensional magnitude is smaller than the dimension of the target. It is also important to note that the qualitative differences in the differential TSOM images for various dimensional changes (e.g., linewidth vs. line height) are much stronger than the differences in the differential TSOM images for various magnitudes of change in the same dimensional parameter (1 nm vs. 2 nm linewidths).

3.4 Integrated Optical Intensity of a Differential TSOM Image Indicates the Magnitude of the Dimensional Difference

Integrated optical intensity of a differential TSOM image can be evaluated in various ways. In the current work, we use two methods. Both can be used to quantify the magnitude of the difference for a single parameter. The first method is the “mean square difference” (*MSD*), which is defined here as,

$$MSD_{AB} = \frac{1}{N} \sum_{i=1}^N (A_i - B_i)^2$$

Where A and B are the TSOM images from two targets, and n is the total number of pixels in the image. Differences of 2.0 nm and 4.0 nm in the linewidths of an isolated line (Fig. 6) produce *MSD* values of 10.0×10^{-6} and 35.0×10^{-6} , respectively. Similarly, 2.0 nm and 4.0 nm differences in the line heights, as shown in Fig. 7, produce *MSD* values of 11.0×10^{-6} and 37.0×10^{-6} , respectively. In these two examples, the *MSD* values increased in direct relationship to the magnitude of the dimensional differences. However, the amount of increase

depends on the individual case. For consistent results and comparison, the total number of pixels in the images, the selected x-axis distance, and the focus range must be kept constant.

The second method is “mean difference” (*MD*), which is defined as follows:

$$MD_{AB} = \frac{1}{N} \sum_{i=1}^N |A_i - B_i|$$

Both *MSD* and *MD* are used appropriately where needed.

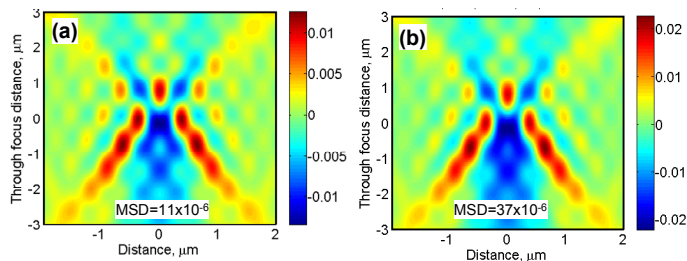


Figure 7. Simulated differential TSOM image obtained for (a) line heights 102 nm and 100 nm (2.0 nm difference), and (b) line heights 104 nm and 100 nm (4.0 nm difference). Isolated line, Line width = 100 nm, Illumination NA = 0.25, Collection NA = 0.95, Illumination wavelength = 546 nm, Si line on Si substrate.

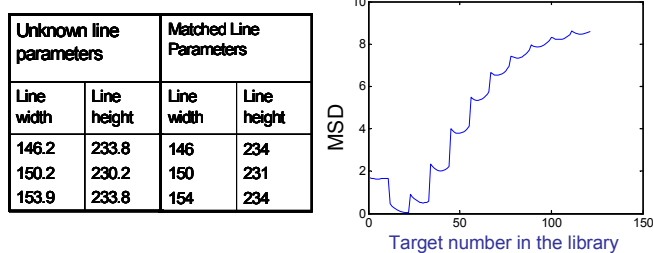


Figure 8. Demonstration of the uniqueness test using simulations. (a) Table showing the unknown line parameters and the matched line parameters from the library. All the dimensions are in nanometers. (b) A typical plot of MSD values evaluated using the library for the simulated unknown target with line width of 146.2 nm and line height of 233.8 nm.

3.5 TSOM Images Appear to be Unique

We tested the uniqueness of TSOM images for a small parameter space using simulations. For this, we simulated a small library of TSOM images for linewidths varying from 145 nm to 155 nm and line heights varying from 125 nm to 135 nm. We used a 1.0 nm step increment for both the linewidth and the line height to produce a total of 121 simulation combinations. We then generated another set of “unknown” target simulations, the dimensions of which do not exactly match that of the targets in the library, as shown in the table in Fig. 8. These “unknown” targets were then compared to the library by evaluating the *MSD* values of their differential TSOM images. A plot of the *MSD* values thus obtained is shown in Fig. 8 for the linewidth of 146.2 nm and the line height of 233.8 nm. The minimum *MSD* value gives the best matched target. The best matched targets for the three unknown targets are also in Fig. 8. The uniqueness and agreement is good for these simulated images, but must yet be verified experimentally.

3.6 TSOM Images are Robust to Optical Aberrations and Process Variation

For metrology applications, it is important to evaluate the robustness of the differential TSOM image method. All optical tools have a degree of optical aberration. Knowing the degree to which

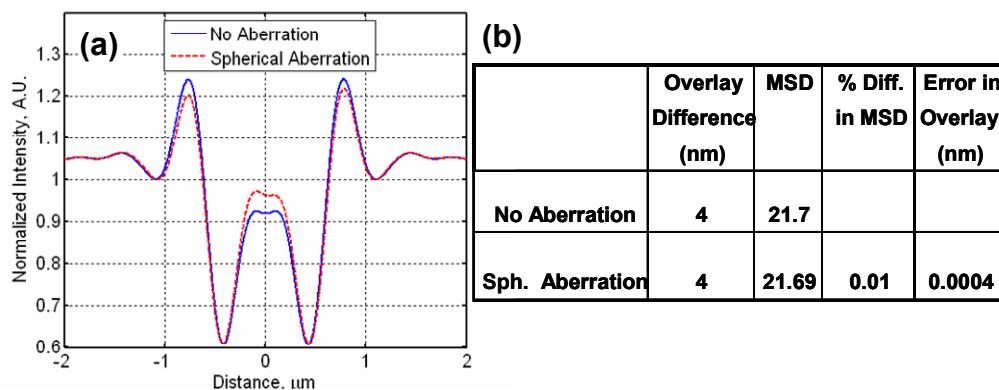


Figure 9. (a) Intensity profiles of NOPI type of in-chip targets with and without spherical aberrations. (b) Table showing error in the overlay measurement due to the presence of spherical aberration. Linewidth = 100 nm, Line height = 100 nm, Trench width = 100 nm, Trench depth = 100 nm; Illumination numerical aperture = 0.27, Collection numerical aperture = 0.8, Wavelength = 546 nm, Electric field perpendicular to the lines.

error is introduced in the measurement by an optical aberration is critical. We studied this using simulations of overlay measurement of an in-chip overlay target, as shown in Fig. 9. TSOM images were simulated under two conditions: without optical aberration and with third order spherical aberration (with Zernike coefficient of 0.01). The optical intensity simulated with the programmed spherical aberration was considerably different from the aberration-free profile.

However, the evaluated *MSD* corresponding to overlay under the two conditions showed a very small variation of about 0.0004 nm for a 4 nm overlay. The error in the overlay measurement is negligible under the experimental conditions, indicating this method is robust to optical aberration as long as the aberration remains constant between the compared TSOM images.

In practice, process variations that produce small changes in the dimensions of the metrology targets are common, including for overlay measurement targets [11]. For a 4 nm overlay, the selected target in Reference 11 produced an *MSD* value of 21.7×10^{-6} . A 5 nm change in the line height due to process variations produced an *MSD* value of 22.3×10^{-6} , which results in a 0.06 nm error in the overlay measurement. Similarly, simulated 4 nm difference in the linewidth produced an overlay error of 0.032 nm. This example shows a relatively small error in the overlay measurement due to process variations, and hence makes this method robust for the conditions studied in Reference 11.

4. TWO TYPES OF APPLICATIONS

Currently, based on the characteristics of the TSOM images, we propose two applications of the TSOM method:

- (i) To determine differences in dimensions, and
- (ii) To determine the absolute dimensions of a target

The first type of application, sensitivity to dimensional change, requires a minimum of two targets. For these sensitivity measurements, although simulations are not necessary, they can greatly enhance the understanding of the dimensional sensitivity behavior pattern of the method.

In the second type of application, an acquired TSOM image is compared with either a simulated or experimentally created library. The best matched TSOM image in the library provides the physical dimensions of the target. Creating a library experimentally requires a set of reference calibration samples (accurately measured with other reference techniques) that span the range of anticipated values for the parameters to be measured by TSOM. Determining the physical dimensions using simulated library, on the other hand, requires accurate simulations, validated by satisfactory experiment-to-simulation agreement during the development phase. In the current work, three types of optical simulation programs were used [4-6], but rigorous experiment to simulation matching has not yet been generally demonstrated.

5. OPTIMIZATION

The sensitivity of a given measurement can be enhanced by optimizing experimental parameters such as polarization, wavelength, illumination, and collection numerical apertures. The polarization state of the illumination produces different sensitivities for a given dimensional difference. This is illustrated in Reference [8] for an isolated line at $\lambda = 193$ nm and 100 nm nominal line height and linewidth for unpolarized, TE-polarized (electric field pointing along the lines), and TM-polarized (electric field pointing perpendicular to the lines) illumination. The results show a large difference in the *MSD* values (i.e., sensitivity) depending on the illumination polarization for a 2.0 nm difference in the line height. Under the given simulation conditions, the TM polarization produced the maximum sensitivity, about 10 times the sensitivity of unpolarized light. Similarly one can optimize the experimental conditions, such as illumination numerical aperture or collection numerical aperture, to produce a maximum sensitivity [8].

6. MEASUREMENT TO SIMULATION COMPARISON

To validate the simulations, data were collected to produce an experimental TSOM image. For this experiment, a Si line grating was chosen and the target and through-focus images were acquired at 100 nm through-focus step increments. Using reference metrology tools such as scanning electron microscopy (SEM) and atomic force microscopy (AFM), the target bottom linewidth, line height, and pitch were measured as 152 nm, 230 nm, and 601 nm, respectively. These were used as input parameters to the model to simulate the TSOM image. The experimental and simulated TSOM images are presented in Fig. 10, demonstrating good qualitative experiment to simulation agreement.

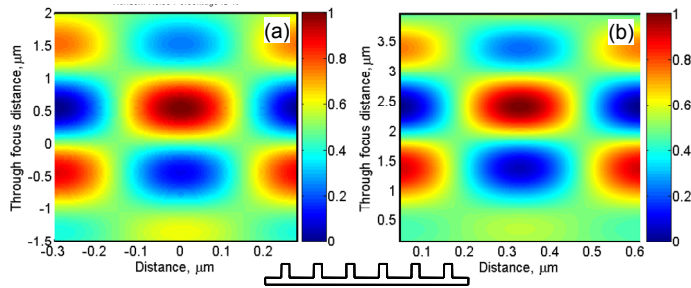


Figure 10. Comparison of (a) simulation, and (b) experimental TSOM images for a line grating. Linewidth = 152 nm, Line height = 230 nm, Pitch = 601 nm, Illumination NA = 0.36, Collection NA = 0.8, Illumination wavelength = 546 nm, Si line on Si substrate. Only one pitch period is shown in the figure.

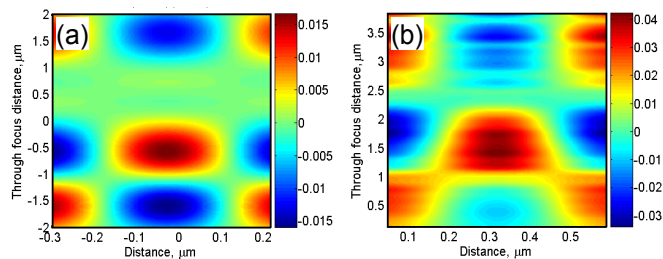


Figure 11. Comparison of (a) simulation and (b) experimental differential TSOM images. The differential images were obtained for the two targets with linewidths of 146 nm and 149 nm. Line height = 230 nm, Pitch = 601 nm, Illumination NA = 0.36, Collection NA = 0.8, Illumination wavelength = 546 nm, Si line on Si substrate.

7. SOME EXAMPLE APPLICATIONS

7.1 Experimental Linewidth Determination Using Simulated Library

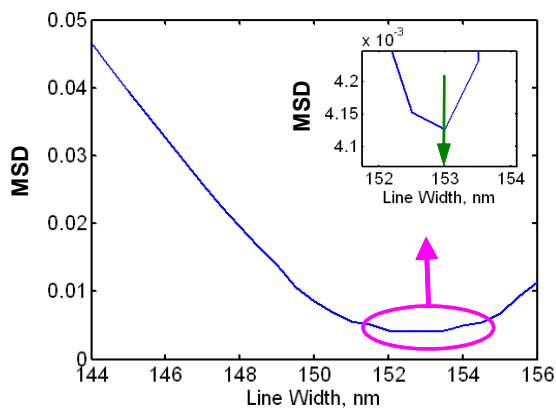


Figure 12. A plot of the MSD values evaluated comparing the experimental 'unknown' target with the library of simulations. The inset shows the magnified portion of the highlighted curve.

The measured differential TSOM image, which includes noise and other experimental imperfections, was compared with the simulation analysis. We chose two line gratings (pitch = 601 nm) with 146 nm and 149 nm linewidths (about 3 nm difference). Using $\lambda = 546$ nm light, we obtained two experimental TSOM images to yield one differential TSOM image. To obtain the experimental differential TSOM image, we normalize the intensities of the experimental TSOM images such that the maximum intensity in the image is equal to one and the minimum intensity equals to zero. The two normalized TSOM images are then cross-correlated to get the best match. At this point, differential TSOM images are obtained. We applied the same normalization procedure to the simulation results to maintain consistency with the experiment. Differential TSOM images from the simulations and the experiments are shown in Fig. 11. Although agreement is not ideal, the images have substantial qualitative similarities.

The utility of the TSOM image approach in metrology is based on an assumption that any given target produces a unique TSOM image under a given experimental condition. A preliminary test to study the uniqueness of the TSOM image using simulations supports (but does not conclusively prove) the assumption as shown in the earlier sections [8].

We applied the same technique to experimentally measure the linewidth of the line grating target shown in Fig. 10(b). The results are still preliminary. We evaluated the dimensions of the selected target, including the linewidth, using an AFM as the reference metrology tool. The AFM-measured linewidth was 145 nm for the selected target. However, we assumed the linewidth to be unknown. Using the measured dimensions, we simulated a small library of TSOM images, varying only the linewidth from 140 nm to 160 nm with a step increment of 0.5 nm, keeping the line height (230 nm), the pitch (601 nm), and the sidewall angle (which is curved) constant. The library matching of the experimental TSOM image (Fig. 10(b)) was carried out by evaluating the *MSD* values from the differential TSOM

images. The differential TSOM images between the experimental and the simulated TSOM images were obtained after they were aligned to get the best correlation. A plot of the *MSD* values evaluated as a function of the linewidth in the library is shown in Fig. 12. The inset shows a magnified view of the minimum of the curve. This gives the best linewidth match as 153 nm. The TSOM image-based linewidth value differs with the AFM measured linewidth of 145 nm. The discrepancy between the AFM and the optical technique requires further study beyond the scope of this paper. However, this example demonstrates the potential utility of the TSOM method for absolute dimensional measurements.

7.2 Dimensional Analysis of Nanodots (Nanoparticles, Quantum Dots) Using Experimental Library

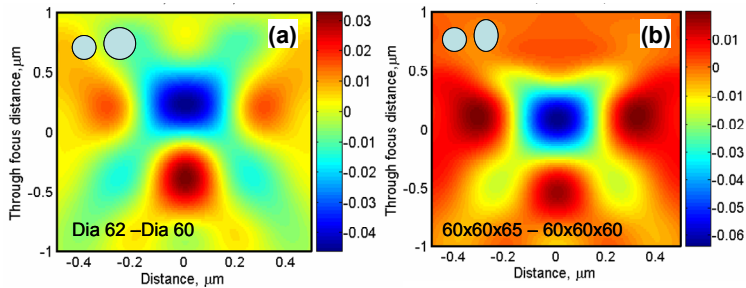


Fig. 13. Simulated differential TSOM images for (a) the size difference of 2.0 nm in diameter (62.0 nm and 60.0 nm), and (b) the shape difference as a result of 5.0 nm elongation in the height. Illumination NA = 0.3, Collection NA = 0.95, Illumination wavelength = 365 nm, Gold particle on quartz substrate.

An important characteristic of TSOM imaging is the ability to differentiate different dimensional changes. This is also applicable to nanoparticle analysis. Figure 13 (a) shows a differential TSOM image for 2 nm difference in the size (diameter) of a nanoparticle. Compare this with the differential TSOM image in Fig. 13 (b) for a difference in the shape (ellipsoid to sphere). We can see that a size difference has a distinct differential image from the shape difference.

We conducted an experiment to determine the size of nanodots using a measured library.

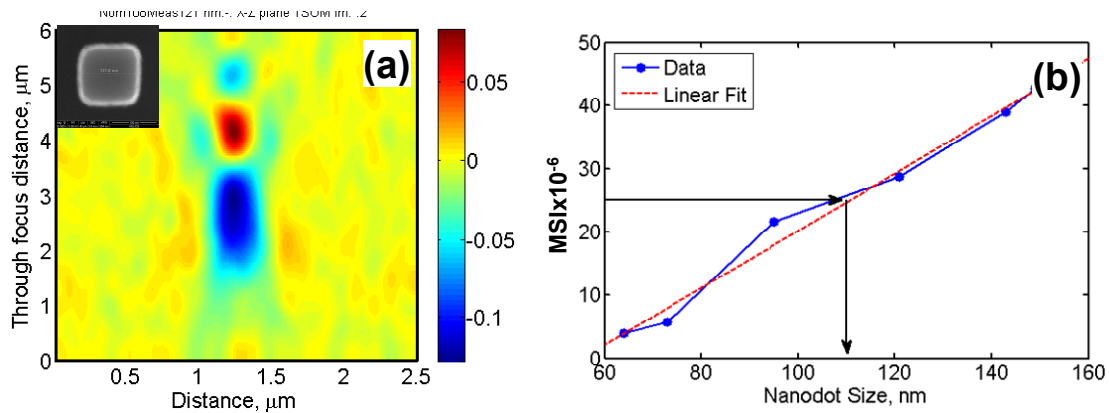


Figure 14. (a) SEM image of a 121 nm nanodot and its experimental intensity-normalized TSOM image (Wavelength = 546 nm, TE Polarization, Illumination NA = 0.27, Collection NA = 0.8, Si nanodot on Si substrate). (b) Experimental mean square intensities of the normalized TSOM images of the selected square nanodots showing a linear trend with size. Arrow marks indicate the experimental size determination of a nanodot of unknown size using the library/calibration curve.

For this purpose, approximately square Si nanodots on a Si substrate were fabricated with nominal sizes ranging from 40 nm to 150 nm and a fixed height of about 70 nm. The SEM lateral dimension reference measurements were always larger than the nominal designed dimensions. Even though the nanodots are not exactly the same as nanoparticles, the measurement procedure remains the same. Lateral dimensions of the nanodots were measured using an SEM, which has a nominal measurement uncertainty of about 5%. Following the SEM measurements, the TSOM images were acquired for the selected nanodots using polarized illumination at a wavelength of 546 nm. A typical background intensity-normalized to zero TSOM image for TE polarization is shown in Fig. 14(a). Using the experimental TSOM images thus created, integrated mean square intensities (MSIs) for the selected nanodots were evaluated and plotted as a function of the SEM-measured nanodot size as shown in Fig. 14(b). Under the current experimental conditions, the curve nominally follows a linear trend. This is treated as the library or the calibration curve for dimensional analysis of nanodots of

unknown size. An “unknown-size” nanodot was measured from this calibration curve using the integrated mean square intensity of its TSOM image, producing a measured size of 108 nm. This “unknown-size” nanodot had previously been measured with SEM producing an measured size of 103 nm. Considering this an initial attempt, the agreement is good.

7.3 CD Analysis of Dense Line Gratings

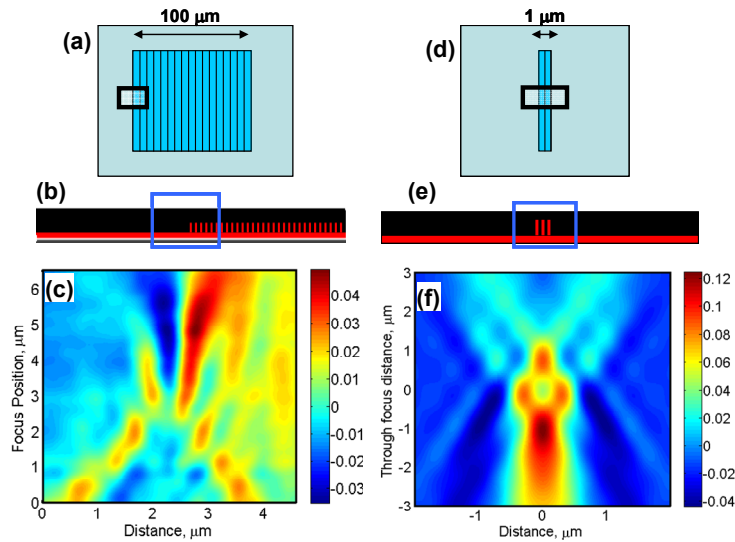


Figure 15. (a) and (b) Location of TSOM analysis for large dense gratings shown in two views. (c) Experimental differential TSOM image at the edge for 3.2 nm difference in the CD using $\lambda = 546$ nm (AFM measured CDs are 118.5 nm and 115.2 nm, Pitch = 300 nm and Line height = 230 nm, Illumination NA = 0.27, Collection NA = 0.8), (d) and (e) Proposed smaller area line gratings shown in two views, and (f) Simulated differential TSOM image for one nanometer difference in the line width using $\lambda = 546$ nm (Linewidths = 17 nm and 16 nm, Pitch = 48 nm (1:2) and Line height = 60 nm)

Although dense, uniform line gratings with pitch below one-half the wavelength of the illumination result in an uninteresting featureless TSOM image when the grating fills the field of view, CD analysis with TSOM is still possible if the edge of the grating is analyzed as shown in Fig. 15(a-c). It is recognized that the dimensions of the lines at the edge of a grating are usually different from the lines in the middle of the grating, however, this does demonstrate a way to use the TSOM method to access some potentially-useful dimensional analysis information, even for dense gratings. The experimental differential TSOM image for an AFM-measured 3.2 nm difference in the linewidths shows a good signal (see Fig. 15(c)). Consequently, we proposed a much smaller size line grating as shown in Fig. 15(d) for dimensional analysis. The simulated differential TSOM image for a nanometer difference in the linewidths shows a good signal (Fig. 15(f)), indicating that the smaller sized gratings are equally effective for dimensional analysis using the TSOM method. Advantages include the ability to use much smaller sized gratings, which use less valuable area, and the ability to extend the use of visible wavelength illumination and optics for measuring dense gratings with linewidths potentially down to as

small as 16 nm (with 1:2 pitch), as listed in the *International Technology Roadmap for Semiconductors* out to 2025. Further experimental verification work is needed to come to a definite conclusion.

7.4 Defect Analysis

Under certain circumstances, the use of the direct (not differential) TSOM image is helpful. For example, TSOM images can highlight the presence of defects and the types of defects in a dense grating, if for example the defect is a periodic variation in linewidth. Experimental TSOM images for four dense gratings fabricated with intentional defects are shown in Fig 16. The four types of defects with periodic 10 nm differences in the linewidths produce distinctly different TSOM images, indicating the presence of the defects and pointing to the type. In contrast, the absence of any defects would produce featureless TSOM images for these dense targets.

Defect analysis is also possible using differential TSOM on isolated line defects in an array of lines, e.g., for a 2 nm reduction in the linewidth as shown in Fig. 17; or defects in a 3D random structure as shown in Fig. 18.

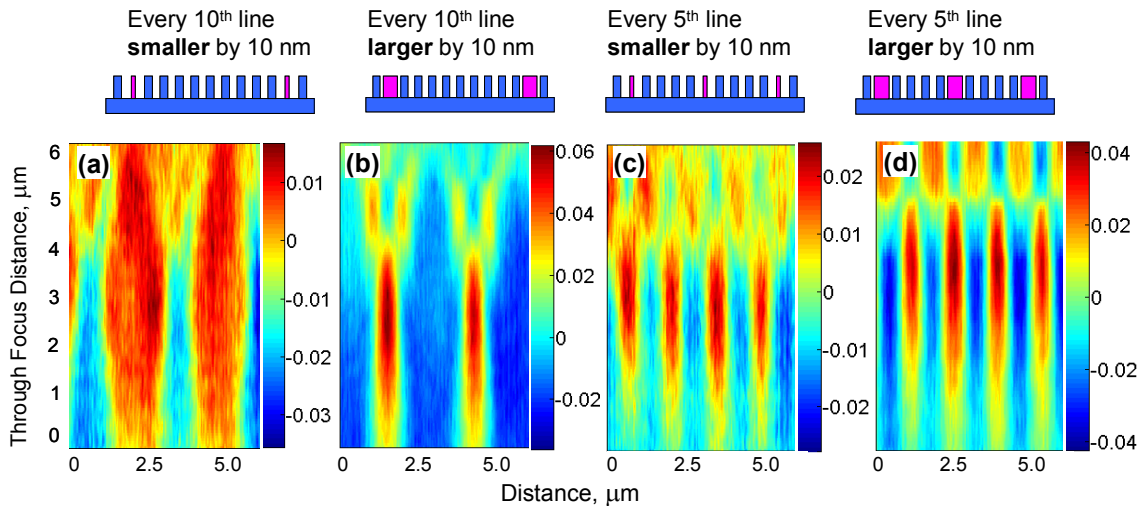


Figure 16. Experimental TSOM images for dense line gratings fabricated with intentional defects. $\lambda = 546$ nm, nominal line width = 100 nm, nominal pitch = 300 nm, illumination NA = 0.36, imaging NA = 0.8.

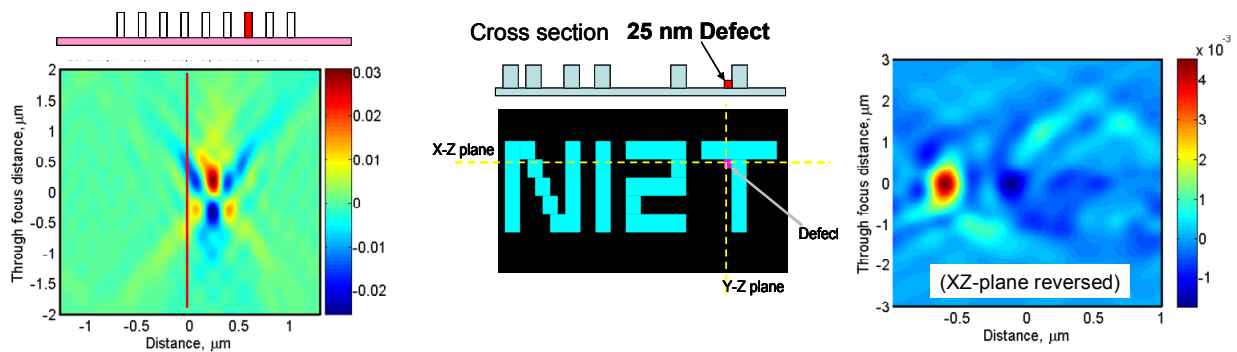


Figure 17. Simulated differential TSOM image showing the presence of a single line defect that is 2 nm smaller than the other linewidths in a dense finite grating. LW = 35 nm, LH = 100 nm, Pitch = 105 nm, Illumination NA = 0.3, Collection NA = 0.8, Total number of lines simulated = 9, Illumination wavelength = 193 nm, Si line on Si substrate.

Figure 18. Determination of the presence of defects in a 3D random structure. (a) Simulated random 3D structure showing a 25 nm defect at the bottom of the features. (b) Simulated differential TSOM image at the x - z plane showing the presence of defect. (Feature linewidth = 100 nm, Line height = 100 nm, $\lambda = 365$ nm, Si features on Si Substrate, Illumination NA = 0.1, Collection NA = 0.8.

7.5 Dimensional Analysis of Through-Silicon Vias (TSVs)

TSVs require truly 3D metrology tools for dimensional analysis as they extend as deep as 50 μm with diameters as large as 5 μm . The TSOM method is ideally suited for dimensional analysis of large targets such as TSVs. Simulated differential TSOM images for diameter and depth change are shown in Fig. 19. As expected, a change in diameter (Fig. 19(a)) results in a distinctly different signal than a change in depth (Fig. 19(b)). Based on the signal strength in these simulated differential images, it may be possible to detect changes as small as a few nanometers in the diameter and depth of 5 μm diameter and 25 μm deep TSVs. Similar type of defect analysis could be applied to MEMS devices.

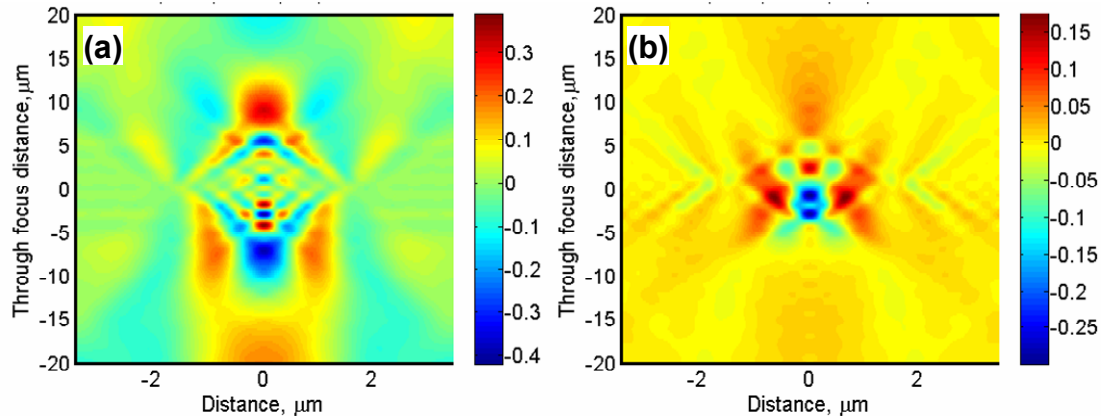


Figure 19. Simulated differential TSOM images for through-silicon vias (TSVs) (a) for 20 nm difference in the diameter, and (b) 20 nm difference in the depth of 5 μm diameter and 25 μm deep through-silicon via using $\lambda = 546$ nm.

7.6 Photomask Dimensional Analysis in Transmission Mode

The TSOM method is equally effective in optical transmission mode for analyzing transparent or relatively small targets on a transparent substrate. For example, we simulated the analysis of photomask features using an optical microscope in transmission mode. Using simulations, we optimized the process to get the maximum sensitivity. The photomask target has an isolated chrome line on a quartz substrate. The linewidth and the line height of this line are 120 nm and 100 nm, respectively. We optimize sensitivity as determined by the *MSD* value for a 2.0 nm difference in the linewidth and height as a function of the polarization and illumination NA as shown in Fig. 20. Under the given simulation conditions, a low 0.1 illumination NA produces high sensitivity for both the linewidth and height variations. However, the linewidth exhibits the highest sensitivity with TE illumination polarization, whereas the line height shows the highest sensitivity with TM illumination polarization.

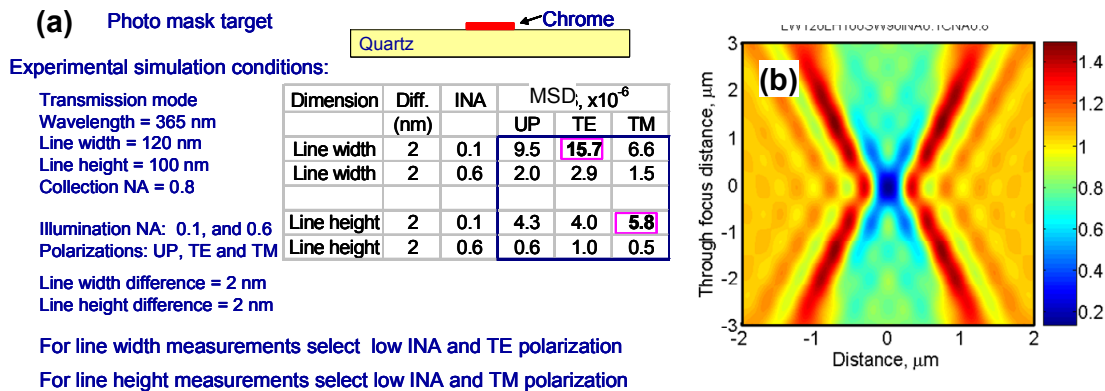


Figure 20. (a) Optimization table for measurement sensitivity (maximize the MSD value) for a photo mask target in transmission microscope mode. (b) A typical TSOM image for a photo mask with dimensions shown in (a).

7.7 Overlay Analysis for Double Patterning

An overlay target was designed for double patterning. Using both simulations and experimental measurements, the TSOM method demonstrated the potential for near 0.1-nm measurement resolution. The design consists of line gratings with alternate lines formed during two process steps. The complete overlay target consists of at least five adjacent gratings with five designed overlay offsets as shown in Fig. 21(a). A simulated TSOM image of such an overlay target is

shown in Fig. 21(b) for zero process overlay. Optical contrast of the TSOM image increases with a greater overlay offset. The TSOM image changes as shown in Fig. 21(c) for a 2 nm process overlay offset. Optical intensities can be integrated (e.g., using *MSD*) in each designed overlay section of the target and plotted as a function of the designed overlay offset as shown in Fig. 21(d). In these plots, the minimum point indicates the process overlay offset.

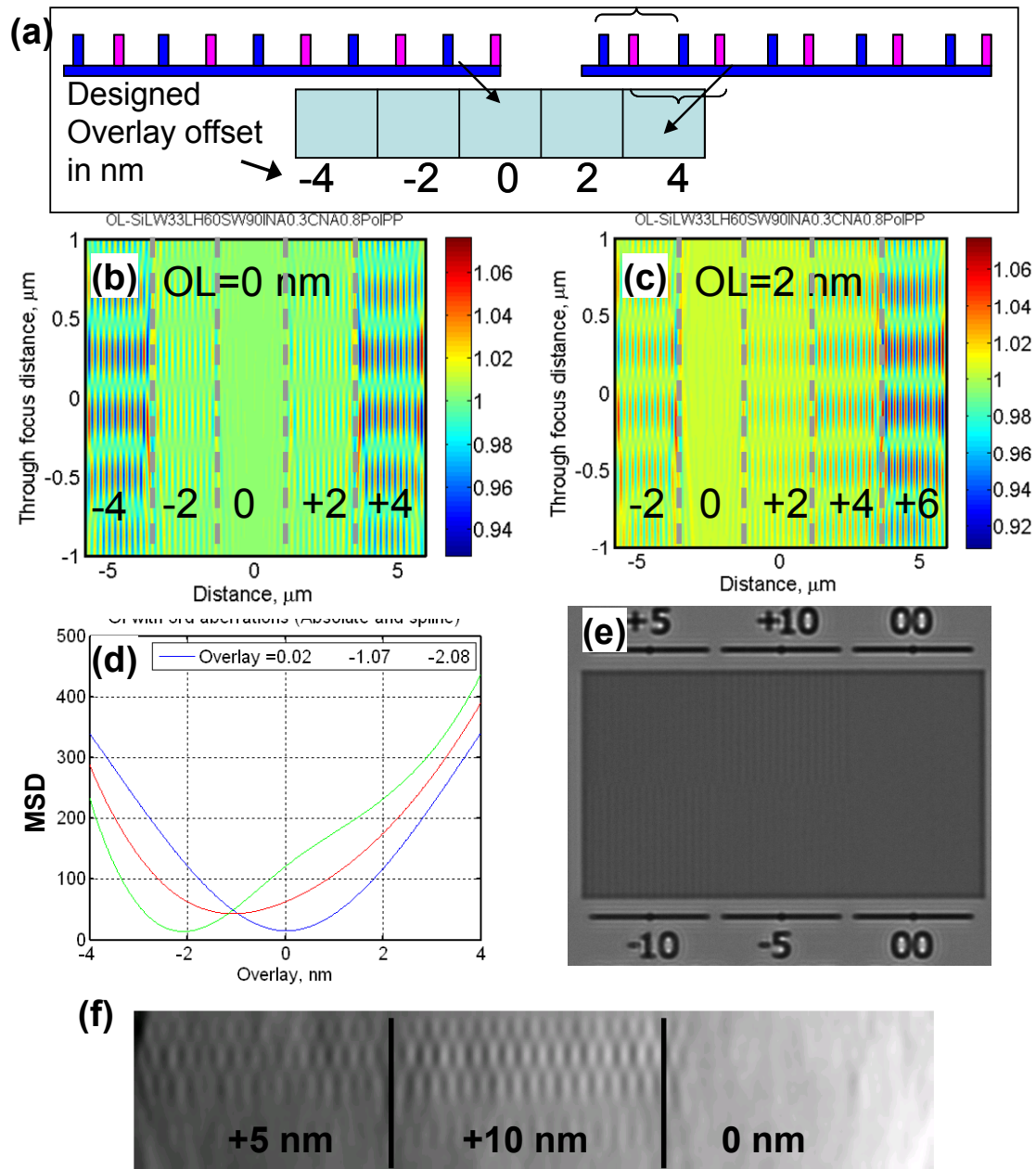


Figure 21. (a) Composite overlay target design composed of multiple designed overlay offsets as indicated for double patterning. Simulated TSOM images of the composite overlay target for (b) zero and (c) 2 nanometer overlay offsets showing increased image contrast with increased overlay offsets ($\lambda = 193 \text{ nm}$). (d) A plot of integrated optical intensities (MSD) as a function of overlay offset (from simulations). Experimentally acquired (e) optical image and (f) TSOM image of a composite overlay target using $\lambda = 546 \text{ nm}$ (designed overlay offsets shown are in nm).

Overlay targets were fabricated based on the composite overlay design. A typical optical image of one such experimental composite overlay target is shown in Fig. 21(e) for zero process overlay, showing very little signal. The measured TSOM image using such a target is shown in Fig. 21(f). As expected, optical contrast increases with greater overlay and validates the simulation results. The composite overlay targets are self-calibrating, robust to process variations and optical aberrations, and highly sensitive, potentially providing near 0.1-nm overlay measurement resolution for double or multiple patterned process applications. TSOM-based analysis for other types of overlay targets can be found in Ref. [11].

8. OPTICAL MODELS

For most of the simulation work presented here, a finite difference time domain (FDTD) optical model was used [5]. This model can simulate 3D targets. On a limited basis, a second, rigorous coupled waveguide analysis (RCWA) optical model [4] was employed. The RCWA model can simulate only 2D targets. 3D optical modeling is computationally intensive. Depending on the size of the simulation domain, grid size, and accuracy required, a 3D simulation with an FDTD model using a high end desktop computer can take as little as a few hours to several days. The optical models used here have been thoroughly studied and compared in-house to evaluate their accuracy.

In the current work, optical modeling may not be required for process control-type applications, as it generally uses differential TSOM imaging. However, the accuracy of the optical simulations is of paramount importance for the second type of application, in which an experimental TSOM image is compared with a library of simulations for direct dimensional measurement. In addition, a thorough quantification of the optical microscope, such as illumination numerical aperture, collection numerical aperture, satisfactory Kohler illumination, and uniformity of illumination across the field of view, etc. is also needed for this application. In addition, optical constants of the target materials must be accurately determined.

9. SUMMARY

This paper presents a novel through-focus scanning optical microscopy (TSOM) method that potentially transforms a conventional optical microscope into a 3D metrology tool with nanometer measurement sensitivity, comparable to typical scatterometry, SEM, and AFM. It achieves this by using the additional information contained in a set of through-focus optical images rather than just a single image at the best focus position. The TSOM images are formed by stacking the through-focus optical image intensity profiles such that the x -axis represents the lateral distance on the target, the y -axis represents the through-focus position and the intensity of the image, and the z -axis represents the optical intensity. We have proposed two main applications of the TSOM images: (i) to determine a change in the relative dimensions and (ii) to determine the actual dimensions of a target. We presented several examples using optical simulations and experimental results.

Differential TSOM images appear to be distinct for different parametric changes. They enable us to identify which parameter is different between two targets. However, the differential TSOM images obtained for different magnitude changes of the same parameter appear qualitatively similar. In this case, the MSD value enables us to determine the magnitude of the difference in the dimension. The TSOM images enable us to determine the dimensions of an unknown target by the library matching method, if we are able to generate accurate simulations and verified by experimental measurement results for a fully characterized optical microscope. We expect the TSOM method to be applicable to a wide variety of targets with a variety of applications including, but not limited to, CD metrology, overlay metrology, defect analysis, inspection, and process control.

10. ACKNOWLEDGEMENTS

The NIST Office of Microelectronics Programs, and an Exploratory Project from the Manufacturing Engineering Laboratory, are gratefully acknowledged for financial support. The authors thank SEMATECH and CNST of NIST for target fabrication and measurement support; Richard Silver for permitting us to use NIST's optical microscope and for helpful discussions during through-focus focus metric studies; and Thomas Germer, Michael Stocker, Bryan Barnes, and Yeung Joon Sohn for their direct or indirect assistance and helpful discussions.

11. REFERENCES

- [1] Instrumentation and Metrology for Nanotechnology, Report of the National Nanotechnology Initiative (2004), http://www.nano.gov/NNI_Instrumentation_Metrology_rpt.pdf.
- [2] Lojkowski W, Turan R, Proykova A, and Daniszewska A 2006 Nanometrology. Eighth Nanoforum Report Nanoforum, http://www.nano.org.uk/members/MembersReports/NANOMETROLOGY_Report.pdf.
- [3] Schwenke H, Neuschaefer-Rube U, Pfeifer T, and Kunzmann H, Optical Methods for Dimensional Metrology in Production Engineering: Annals of the CIRP (Elsevier) 51 685-98 (2002).
- [4] Mark Davidson, "Analytic waveguide solutions and the coherence probe microscope," Microelectronic Engineering 13 523-26 (1991).
- [5] T.V. Pistor, 2001 Electromagnetic Simulation and Modeling with Applications in Lithography, Ph.D. Thesis Memorandum No. UCB/ERL M01/19.
- [6] Germer, T., and Marx, E. Proc. SPIE 6152, 61520I1, (2006).
- [7] Attota, R., Silver R.M., and Potzick, J., "Optical illumination and critical dimension analysis using the through-focus focus metric," Proc. SPIE, 6289, p. 6289Q-1-10 (2006).
- [8] Attota, R., Silver, R.M., and Barnes, B.M., "Optical through-focus technique that differentiates small changes in line width, line height, and sidewall angle for CD, overlay, and defect metrology applications," Proc. SPIE 6922, 6922OE-1-13, (2008).
- [9] Brown, E., "Nanoscale Dimensioning Is Fast, Cheap with New NIST Optical Technique," NIST Tech Beat, October 28, http://www.nist.gov/public_affairs/techbeat/tb2008_1028.htm#tsom (2008).
- [10] Attota, R., Germer, T.A., and Silver, R.M., "Through-focus scanning-optical-microscope imaging method for nanoscale dimensional analysis," Optics Letters, Vol. 33, Issue 17, pp. 1990-1992 (2008).
- [11] Attota, R.; Stocker, M., Silver, R.M., Alan Heckert; Hui Zhou; Richard Kasica; Lei Chen; Ronald Dixon; George Orji; Barnes, B.M., Peter Lipscomb, "Through-focus scanning and scatterfield optical methods for advanced overlay target analysis," Proc. SPIE Int. Soc. Opt. Eng. 7272, 727214, (2009).
- [12] Attota, R., Germer, T.A., and Silver, R.M., "Nanoscale measurements with a through-focus scanning optical microscope," Future Fab, 30, pp 83-88, (2009).
- [13] Attota, R., and Silver, R.M., "Nanometrology using a through-focus scanning optical microscopy method," Meas. Sci. Technol. 22 , pp 024002, (2011).
- [14] Attota, R., "Nanoscale Measurements with the TSOM Optical Method," an on-line presentation from NIST, (2011), <http://www.nist.gov/pml/div681/grp14/upload/tsom-ravikiran-attota.pdf>.
- [15] N.S. Levine, T.R. Corle, R.T. Mumaw, C-H Chou, and G.S. Kino, Multilevel CD/Overlay metrology using a real-time confocal scanning optical microscope," Microelectronic Engineering 11, 669-674, (1990).
- [16] Attota, R., Silver, R.M., Germer, T.A., Bishop, M., Larrabee, R., Stocker, M., and Howard, L., "Application of through-focus focus-metric analysis in high resolution optical metrology," Proc. SPIE, 5752, 1441 (2005).
- [17] Silver, R.M., Barnes, B.M., Attota, R., Jun, J., Stocker, M., Marx, E., and Patrick, H.J., "Scatterfield microscopy for extending the limits of image-based optical metrology," Applied Optics, Vol. 46, Issue 20, pp. 4248-4257 (2007).
- [18] Germer, T.A., and Marx, E., "Simulations of optical microscope images", Proc. SPIE 6152, 61520I (2006).
- [19] Silver, R.M., Barnes, B.M., Sohn, Y. Quintanilha, R., Hui Zhou, Chris Deeb, Mark Johnson, Milton Goodwin and Dilip Patel, "The limits and extensibility of optical patterned defect inspection", Proc. SPIE 7638, 76380J (2010).